JOURNAL OF GEOPHYSICAL RESEARCH, VOL. 93, NO. A7, PAGES 7515–7520, JULY 1, 1988

# Ordinary Mode Auroral Kilometric Radiation Fine Structure Observed by DE 1

ROBERT F. BENSON

*Laboratory for Extraterrestrial Physics, NASA Goddard Space Flight Center, Greenbelt, Maryland*

MARY M. MELLOTT, RICHARD L. HUFF, AND DONALD A. GURNETT

*Department of Physics and Astronomy, University of Iowa, Iowa City*

The fine structure observed with intense right-hand extraordinary (*R-X*) mode auroral kilometric radiation (AKR) has received major theoretical attention. Data from the Dynamics Explorer 1 plasma wave instrument indicate that left-hand ordinary (*L-O*) mode AKR possesses similar fine structure. Several theories have been proposed to explain the fine structure of the *R-X* mode AKR. In order to account for the *L-O* mode fine structure, these theories will have to be modified to produce the *L-O* mode directly or will have to rely on mode conversion processes from the *R-X* to the *L-O* mode.

## INTRODUCTION

The identification of the Earth as a radio planet was first convincingly demonstrated by *Gurnett* [1974]. The terrestrial radiation, which was associated with discrete auroral arcs, is now referred to as auroral kilometric radiation (AKR). *Gurnett et al.* [1979] and *Gurnett and Anderson* [1981] used ISEE 1 and 2 wideband data to show that AKR consists of many discrete narrow-band ($\lesssim$1 kHz) emissions. *Morioka et al.* [1981] provided additional evidence of AKR fine structure based on observations from the Jikiken (EXOS-B) satellite; they observed narrow-band (2–5 kHz) spectral peaks superimposed on intense broadband AKR spectra. *Baumback and Calvert* [1987] pointed out that while the apparent bandwidth of most of the discrete AKR emissions observed by ISEE 1 and 2 is about 1 kHz, the bandwidth can be considerably less. They used autocorrelation techniques on the data from one event to resolve spectral features with bandwidths as low as 5–10 Hz.

Several mechanisms have been suggested to explain the observed AKR fine structure. In view of the observed frequency drift with time for the discrete AKR frequency structures, *Gurnett et al.* [1979], *Gurnett and Anderson* [1981], and *Morioka et al.* [1981] suggested that disturbances traveling along the magnetic field were responsible for the fine structure. *Gurnett and Anderson* [1981] showed that the frequency drift rates corresponded to source motions with speeds close to the ion acoustic speed (assuming that the emission takes place near the electron cyclotron frequency $f_{ce}$). *Grabbe* [1982] interpreted banded features in the ISEE data, separated by the ion cyclotron frequency, in terms of a three-wave coupling involving electrostatic ion cyclotron waves. *Le Queau et al.* [1985] showed that if such waves give rise to coherent electron density fluctuations near the wave reflection point, then the observed AKR frequency modulation with frequency spacings equal to the ion cyclotron frequency would be expected. Their analysis was based on a treatment of the cyclotron maser instability, initially proposed by *Wu and Lee* [1979] to explain AKR, that included the effect of inhomogeneity along the geomagnetic field lines. The discrete fine structure spectrum of AKR is a natural consequence of the feedback model proposed by *Calvert* [1982]. The emission mechanism in this case is analogous to an optical laser oscillator. *Melrose* [1986] introduced a phase-bunching mechanism specifically to explain the fine structure observed in AKR and in the Jovian decametric radiation. It represents a modification of the feedback model of *Helliwell* [1967] for discrete VLF emissions.

The models proposed by *Calvert* [1982] and *Melrose* [1986] to explain the AKR fine structure considered the direct generation of right-hand extraordinary (*R-X*) mode radiation. The observations to be presented here, however, indicate that fine structure is present in left-hand ordinary (*L-O*) mode AKR as well as *R-X* mode AKR. *Calvert* [1982] proposed that any *L-O* mode AKR would be produced as a by-product of intense *R-X* mode AKR due to a polarization mismatch at the source boundary.

Ordinary mode AKR has been observed by at least eight different spacecraft. Three of these made direct polarization measurements, namely, Voyager 1 and 2 [*Kaiser et al.*, 1978] and DE 1 [*Shawhan and Gurnett*, 1982; *Mellott et al.*, 1984]. Ordinary mode AKR was inferred from four spacecraft on the basis of wave cutoff effects (Hawkeye and ISEE 1 [*Calvert*, 1982], Jikiken [*Oya and Morioka*, 1983], and ISIS 1 [*Benson*, 1984, 1985]). Polarization determinations from the Viking satellite were based on wave cutoffs and signal intensity measurements by *Bahnsen et al.* [1987] and on wave cutoffs and spin modulation patterns by *de Feraudy et al.* [1987]. The next two sections will be devoted to a presentation of wideband DE 1 observations showing *L-O* mode fine structure and the resulting theoretical implications.

## OBSERVATIONS

The DE 1 plasma wave instrument (PWI) [*Shawhan et al.*, 1981] is ideal for the investigation of AKR because it provides the capability of (1) measuring wave polarization [*Shawhan and Gurnett*, 1982; *Mellott et al.*, 1984], (2) determining the direction of arrival [*Calvert*, 1985; *Mellott et al.*, 1985], and (3) providing wideband data as was done on ISEE 1 by *Gurnett et al.* [1979]. The present work will emphasize the first and third instrumental capabilities to illustrate that both *L-O* and *R-X* mode AKR reveal fine structure.



Paper number 7A9312.
0148-0227/88/007A-9312$02.00

Plate 1*a* presents a color electric field spectrogram for a DE 1 pass on April 1, 1983, over the southern auroral zone. AKR is observed above the curved line designating $f_{ce}$. The AKR reveals an increase in intensity and an upward frequency shift near 0355 UT. In this time interval near 0355 UT the AKR lower frequency limit is well above $f_{ce}$ (see the upper curved lines in Plates 1*a* and 1*b*), which indicates that the received signals were generated well below the spacecraft [*Benson and Calvert*, 1979], which was located at a radial distance of more than 4 $R_E$.

The sudden change in signal characteristics near 0355 UT suggests the presence of two independent signals. Upon closer inspection, the average power near 150 kHz is seen to change by approximately 20 dB from 0352 to 0359 UT. This suggestion of two independent signals is given further support by an inspection of the polarization spectrogram shown in Plate 1*b*. The PWI instrument was operating in a mode using the long-wire electric dipole antenna and the magnetic loop antenna. Under these conditions the wave polarization determination requires a knowledge of the direction of wave propagation [*Mellott et al.*, 1984]. As indicated in the previous paragraph, it is reasonable to assume that the waves are propagating upward in this case. On the basis of this assumption, yellow represents *L-O* mode polarization, and purple represents *R-X* mode polarization in Plate 1*b* (the color coding used in the southern hemisphere). It is seen from this polarization spectrogram that the sudden change in signal intensity observed in the electric field spectrogram of Plate 1*a* near 0355 UT corresponds to a transition from predominantly *L-O* mode AKR (yellow) to predominantly *R-X* mode AKR (purple) in the frequency range between 60 and 300 kHz. (Note that the *L-O* and *R-X* mode signals occupy the lower and upper portions of this frequency region, respectively.)

During this *L-O* to *R-X* mode transition time interval the PWI wideband receiver was collecting data from 125 to 165 kHz. Plate 1*c* represents the wideband data obtained during a 30-min sample of the 2-hour data interval of Plates 1*a* and 1*b*. The labels designating "left-hand" and "right-hand" in Plate 1*c* corresponds to the yellow (*L-O* mode) and purple (*R-X* mode) colors in Plate 1*b*, respectively. The frequency range covered in Plate 1*c* corresponds to a sample of the upper frequency portion of *L-O* mode AKR and the lower frequency portion of *R-X* mode AKR in the transition region seen in Plate 1*b*. Thus the last 3 min of *L-O* mode AKR are predominantly below the 125-kHz lower band edge in Plate 1*c* (the *L-O* mode is clearly seen until 0400 UT in Plate 1*b*).

The main features to note in Plate 1*c* are the discrete narrow-band ($\lesssim$1 kHz) frequency structures that drift in frequency with increasing time in both the *L-O* and *R-X* modes. In this particular example the *L-O* mode structures reveal a sharp increase of frequency with increasing time while the *R-X* mode structures show a slower frequency decrease with time. These characteristics, which are not necessarily typical (though a detailed study of this point has not been made), again suggest that the *L-O* and *R-X* mode signals may be independent.

A second example illustrating fine structure in both wave modes is presented in Plate 2. Again, AKR is observed at frequencies above $f_{ce}$, indicating a source region below the spacecraft. In this case the AKR in the electric field spectrogram of Plate 2*a* is not as intense as in the example of Plate 1*a*, and it does not immediately suggest the presence of two independent signals. The polarization spectrogram of Plate 2*b*, on the other hand, does indicate that the AKR in the 50- to 400-kHz range is composed of signals of different polarization. Near the center of the 2-hour time interval displayed in Plate 2*b* there was an instrumental mode change from a configuration using one electric dipole antenna and the magnetic loop antenna to a configuration using the two orthogonal electric dipole antennas. This pass was in the northern hemisphere on September 22, 1981, where the polarization color coding for the first configuration is yellow for the *R-X* mode and purple for the *L-O* mode (assuming they are upgoing waves). (As is pointed out earlier, the observed AKR frequencies above $f_{ce}$ indicate that the waves are propagating upward to the spacecraft.) In the second configuration, i.e., using the two orthogonal electric dipoles (after 0715 UT in Plate 2*b*) where the polarization determination is unambiguous with respect to the direction of wave propagation [*Mellott et al.*, 1984], the color coding used in the northern hemisphere is red for the *R-X* mode and green for the *L-O* mode. The AKR on both sides of this instrumental mode change at 0715 UT is composed of an *L-O* mode signal from about 50 to 160 kHz with a higher-frequency *R-X* mode signal. A comparison with the signal strengths in the electric field spectrogram of Plate 2*a* indicates that the *R-X* mode waves and the *L-O* mode waves are of comparable intensity in this case. For a few minutes around 0730 UT, however, the *R-X* mode waves dominate the *L-O* mode waves in the 100- to 300-kHz frequency range (see the red intrusion into the green trace in Plate 2*b*). (Note that at any given time the polarization is determined by the strongest signals arriving at the antennas.)

The wideband data for a 30-min interval of this event, including the *L-O*/*R-X* mode transition centered near 0730 UT, are presented in Plate 2*c*. The wideband data near 0730 UT labeled "right-hand," corresponding to the red-coded *R-X* mode in Plate 2*b*, reveal both rising and falling frequency structures. The "left-hand" data on each side of the "right-hand" data in Plate 2*c*, corresponding to the green-coded *L-O* mode in Plate 2*b*, show mostly rising tones. Intense *L-O* falling tones are seen, however, between 0722 and 0723 UT and between 0738 and 0739 UT in the frequency range between 125 and 135 kHz. Also, a rising *L-O* signal is seen to "turn around" at 155 kHz at 0739 UT.

While *L-O* mode AKR often appears to exhibit fine structure, cases such as those illustrated in Plates 1*c* and 2*c* showing wave mode transitions in the wideband data are not common. In order to capture such a transition, the wideband receiver must be operating with the proper lower band edge (there are seven possible frequencies ranging from 31.25 to 2000 kHz [*Shawhan et al.*, 1981]) while the predominate AKR being received by DE 1 is changing from one wave mode to another. During the first two years of the DE mission (September 1981 through October 1983), wideband data in one of the appropriate bands for detecting AKR (125 or 250 kHz) were available for approximately 150 satellite passes. An inspection of 46 of these passes, where summary slides with polarization information have been processed, indicated that 18 passes had only *R-X* mode AKR, 11 had only *L-O* mode AKR, and 17 revealed both modes. Fine structure AKR was observed in all cases.

## DISCUSSION

The fine structure in the *L-O* mode AKR presented in the previous section has an important bearing on the theoretical

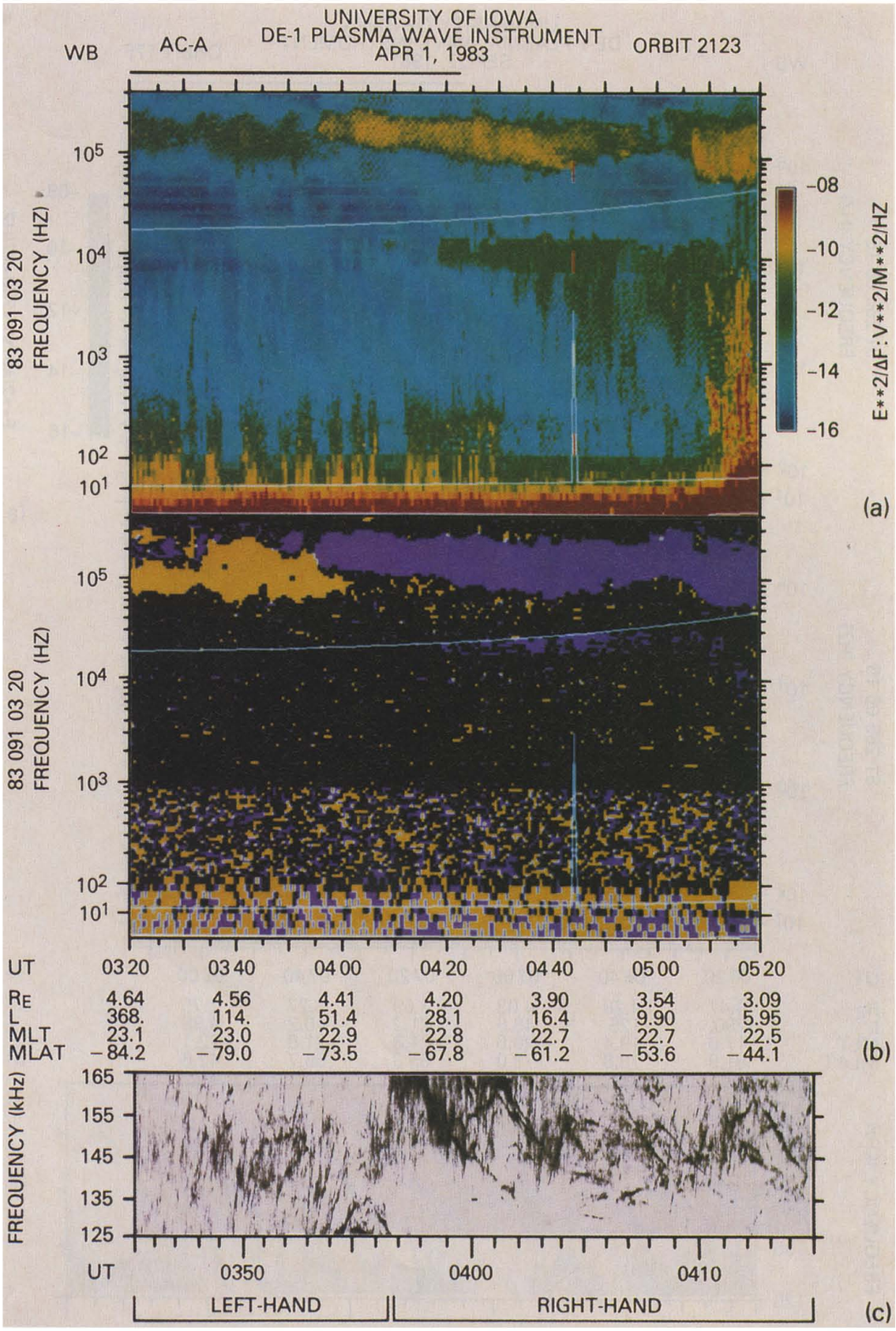


Plate 1. DE 1 (*a*) electric field, (*b*) polarization, and (*c*) electric field wideband spectrograms. In Plates 1*a* and 1*b* the curved white lines represent the local electron (upper) and proton (lower) cyclotron frequencies, and the emissions above $f_{ce}$ correspond to the AKR of interest to the present discussion. In Plate 1*b*, yellow corresponds to *L-O* mode upgoing waves, and purple corresponds to *R-X* mode upgoing waves during this southern hemisphere pass.

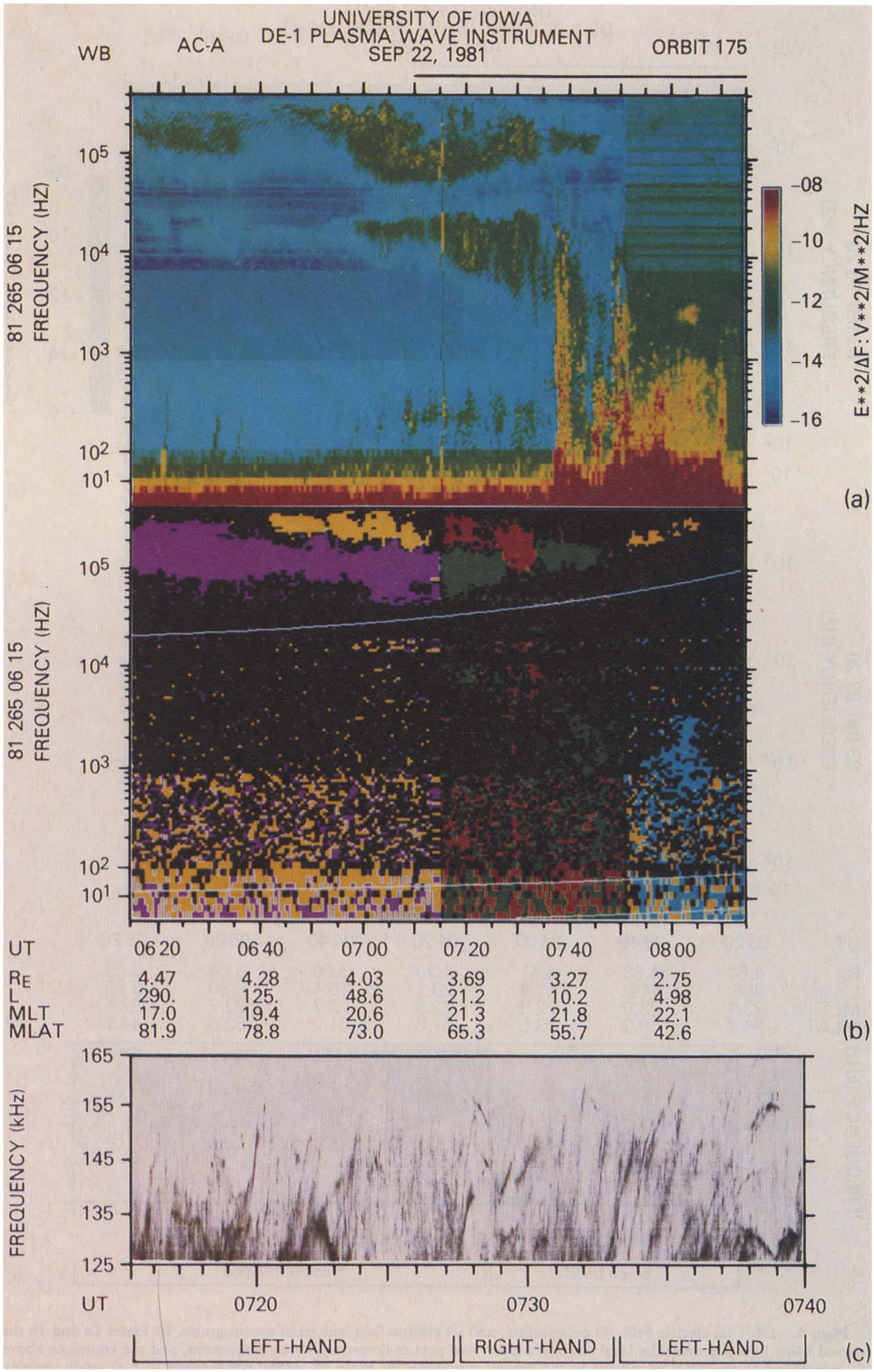


Plate 2. Same as Plate 1 except for a northern hemisphere pass with an instrumental mode change from the EX-B mode to the EX-EZ mode at 0715 UT. In the former case, yellow corresponds to *R-X* mode upgoing waves, and purple corresponds to *L-O* mode upgoing waves; in the latter case, red corresponds to *R-X* mode waves (arriving from either up or down), and green corresponds to *L-O* mode waves (up or down).

interpretation of AKR. In the cyclotron maser mechanism, *R-X* mode AKR dominates over *L-O* mode AKR only in a low-density plasma, i.e., when the electron plasma to cyclotron frequency ratio ($\omega_{pe}/\Omega_e$) is less than about 0.3. When the *L-O* mode dominates over the *R-X* mode, at higher $\omega_{pe}/\Omega_e$ values, it is expected to be much weaker than this intense *R-X* mode from low-density regions on the basis of linear theory [e.g., *Melrose et al.*, 1984]. Major theoretical efforts have been directed toward explaining the fine structure of the *R-X* mode [*Calvert*, 1982; *Melrose*, 1986]. In order to get *L-O* mode AKR from low-density source regions, *R-X* to *L-O* mode conversion at density boundaries was suggested by *Calvert* [1982] and investigated in detail by *Hayes and Melrose* [1986]. Ordinary mode generation based on *Z* to *L-O* mode wave conversion has also been proposed [*Benson*, 1975; *Jones*, 1977; *Oya and Morioka*, 1983; *Jones et al.*, 1984]. The cyclotron maser instability mechanism first proposed by *Wu and Lee* [1979], however, is able to explain the various AKR wave modes observed under different source region plasma conditions [*Benson*, 1985; *Benson and Wong*, 1987] and to enable preencounter predictions of planetary emission [*Curtis*, 1985] that were confirmed after the Voyager 2 Uranian encounter [*Kaiser et al.*, 1987; *Curtis et al.*, 1987; *Desch and Kaiser*, 1987].

The major question pertinent to the present paper, from the point of view of the cyclotron maser mechanism, is whether the *L-O* mode revealing fine structure is the result of a direct generation from relatively high plasma density regions ($\omega_{pe}/\Omega_e \gtrsim 0.3$) or an *R-X* to *L-O* mode conversion at a boundary of a low-density ($\omega_{pe}/\Omega_e \lesssim 0.3$) region. While the present observations do not specifically address this problem, there is observational evidence from several earlier studies to support both the direct and the indirect processes. The ISIS 1 AKR source region observations support the concept of direct *L-O* mode generation in the region outside the AKR plasma density cavity (see Figure 30 and the associated text on pp. 2773 and 2774 of *Benson* [1985]). Additional evidence for direct *L-O* mode generation was provided by the simultaneous detection of fundamental *L-O* mode and second harmonic *R-X* mode AKR by DE 1 [*Mellott et al.*, 1986]. These observations are consistent with the cyclotron maser instability growth rate calculations of *Winglee* [1985] and *Benson and Wong* [1987] which were based on relatively high density conditions ($\omega_{pe}/\Omega_e \gtrsim 0.3$) and perpendicular bump features on the electron distribution function. (These calculations indicated that the maximum temporal growth rates of the fundamental *L-O* mode and second harmonic *R-X* mode are comparable when $\omega_{pe}/\Omega_e \approx 0.4$.) DE 1 observations of highly correlated *R-X* and *L-O* mode signal intensities by *Mellott et al.* [1984], on the other hand, suggest that the *L-O* mode is produced as a by-product from *R-X* mode generation in the AKR cavity, as first proposed by *Calvert* [1982]. Calvert (personal communication, 1987) argues that the simultaneous fundamental *L-O*/second harmonic *R-X* mode DE 1 observations of *Mellott et al.* [1986] also support the by-product mechanism because the fundamental *R-X* mode, being generated near a cutoff conditions, would be expected to be refracted into a different final direction. Observations from the Viking satellite relevant to this process were provided by *de Feraudy et al.* [1987]. They observed a spin modulation phase change in the AKR signals detected by Viking as the spacecraft crossed an AKR cavity which they suggested could be evidence for *R-X* to *L-O* mode conversion. They pointed out, however, that the observations were not consistent with the expected conversion efficiencies predicted by *Hayes and Melrose* [1986].

The present observations do not necessarily imply that the different wave modes observed originated from the same source location. They could have been due to independent signals, from independent sources, arriving at the spacecraft at the same time. ISIS 1 source region observations have indicated that AKR sources are distributed over a wide portion of the nightside auroral region, i.e., about 15° invariant latitude Λ (centered between 65° and 70°Λ), and that they extend over at least 6 hours of magnetic local time (centered between 2200 and 2300 MLT) [*Benson and Calvert*, 1979, Figure 5; *Benson*, 1985, Figures 17*g*, 17*h*, 29*b*, and 29*c*]. Such a wide distribution of AKR is also indicated by the close correlation of AKR to discrete auroral forms [*Gurnett*, 1974; *Benson and Akasofu*, 1984; *Huff et al.*, 1986] since auroral imagers on a half dozen spacecraft have revealed a wide distribution of such bright auroral features throughout the auroral ovals (see, for example, *Anger and Lui* [1973] (ISIS 2), *Akasofu* [1974] (DMSP 2), *Frank et al.* [1982] (DE 1), *Meng and Huffman* [1984] (HILAT), *Shepherd et al.* [1987] (Viking), and *Meng et al.* [1987] (Polar Bear)). The possibility of independent *X* and *O* mode signals from different regions of the auroral oval is also consistent with the predictions of the cyclotron maser mechanism, i.e., *X* mode AKR from low-density source regions and *O* mode AKR from higher-density regions [*Melrose et al.*, 1984; *Winglee*, 1985; *Benson and Wong*, 1987].

The concept of direct generation of *L-O* mode AKR by the cyclotron maser instability received some convincing extraterrestrial support by the Voyager 2 observations at Uranus [*Desch and Kaiser*, 1987]. Ordinary mode Uranian kilometric radiation was only observed to emanate from the dayside of the planet where $\omega_{pe}/\Omega_e \lesssim 1$ conditions were expected on the basis of magnetic field models and radio occultation observations. The *L-O* mode was observed to be much weaker than the nightside *R-X* mode emission originating from a source region where $\omega_{pe}/\Omega_e \lesssim 0.3$ was likely.

The present observations of AKR *L-O* mode fine structure, added to the earlier reports of *R-X* mode fine structure (both emission modes being predicted by the cyclotron maser mechanism), suggest a thorough search of available wideband data for possible fine structure in other aurorally generated emissions attributed to the cyclotron maser mechanism, such as the fundamental *Z* mode, whistler mode, and second harmonic *R-X* and *Z* modes investigated by *Benson and Wong* [1987].

## Summary

Fine frequency structure elements are observed in *L-O* mode AKR that resemble the previously observed *R-X* mode AKR fine structure. There is considerable observational and theoretical evidence that *L-O* mode emissions can be directly generated by the cyclotron maser mechanism. Future theoretical efforts should consider the direct generation of *L-O* mode fine structure in planetary magnetospheres; future observational endeavors should investigate existing wideband data for possible fine structure in other observed wave modes and harmonics predicted by the cyclotron maser mechanism.

*Acknowledgments.* We acknowledge helpful discussions with and useful information from W. Calvert, S. A. Curtis, M. D. Desch, and M. L. Kaiser. Support for the Dynamics Explorer Program at the University of Iowa was through NASA/GSFC NAG5-310.

The Editor thanks H. deFeraudy and D. B. Melrose for their assistance in evaluating this paper.

## REFERENCES


Akasofu, S.-I., A study of auroral displays photographed from the DMSP-2 satellite and from the Alaska meridian chain of stations, *Space Sci. Rev.*, *16*, 617–725, 1974.

Anger, C. D., and A. T. Y. Lui, A global view at the polar region on 18 December 1971, *Planet. Space Sci.*, *21*, 873–878, 1973.

Bahnsen, A., M. Jespersen, E. Ungstrup, and I. B. Iversen, Auroral hiss and kilometric radiation measured from the Viking satellite, *Geophys. Res. Lett.*, *14*, 471–474, 1987.

Baumback, M. M., and W. Calvert, The minimum bandwidths of auroral kilometric radiation, *Geophys. Res. Lett.*, *14*, 119–122, 1987.

Benson, R. F., Source mechanism for terrestrial kilometric radiation, *Geophys. Res. Lett.*, *2*, 52–55, 1975.

Benson, R. F., Ordinary mode auroral kilometric radiation, with harmonics, observed by ISIS 1, *Radio Sci.*, *19*, 543–550, 1984.

Benson, R. F., Auroral kilometric radiation: Wave modes, harmonics, and source region electron density structures, *J. Geophys. Res.*, *90*, 2753–2784, 1985.

Benson, R. F., and S.-I. Akasofu, Auroral kilometric radiation/aurora correlation, *Radio Sci.*, *19*, 527–541, 1984.

Benson, R. F., and W. Calvert, ISIS 1 observations at the source of auroral kilometric radiation, *Geophys. Res. Lett.*, *6*, 479–482, 1979.

Benson, R. F., and H. K. Wong, Low-altitude ISIS 1 observations of auroral radio emissions and their significance to the cyclotron maser instability, *J. Geophys. Res.*, *92*, 1218–1230, 1987.

Calvert, W., A feedback model for the source of auroral kilometric radiation, *J. Geophys. Res.*, *87*, 8199–8214, 1982.

Calvert, W., DE-1 measurements of AKR wave directions, *Geophys. Res. Lett.*, *12*, 381–384, 1985.

Curtis, S. A., Possible nightside source dominance in nonthermal radio emissions from Uranus, *Nature*, *318*, 47–48, 1985.

Curtis, S. A., M. D. Desch, and M. L. Kaiser, The radiation belt origin of Uranus' nightside radio emission, *J. Geophys. Res.*, *92*, 15,199–15,205, 1987.

de Feraudy, H., B. M. Pedersen, A. Bahnsen, and M. Jespersen, Viking observations of auroral kilometric radiation from the plasmasphere to night auroral oval source regions, *Geophys. Res. Lett.*, *14*, 511–514, 1987.

Desch, M. D., and M. L. Kaiser, Ordinary mode radio emission from Uranus, *J. Geophys. Res.*, *92*, 15,211–15,216, 1987.

Frank, L. A., J. D. Craven, J. L. Burch, and J. D. Winningham, Polar views of the Earth's aurora with Dynamics Explorer, *Geophys. Res. Lett.*, *9*, 1001–1004, 1982.

Grabbe, C. L., Theory of the fine structure of auroral kilometric radiation, *Geophys Res. Lett.*, *9*, 155–158, 1982.

Gurnett, D. A., The Earth as a radio source: Terrestrial kilometric radiation, *J. Geophys. Res.*, *79*, 4227–4238, 1974.

Gurnett, D. A., and R. R. Anderson, The kilometric radio emission spectrum: Relationship to auroral acceleration processes, in *Physics of Auroral Arc Formation, Geophys. Monogr. Ser.*, vol. 25, edited by S.-I. Akasofu and J. R. Kan, pp. 341–350, AGU, Washington, D. C., 1981.

Gurnett, D. A., R. R. Anderson, F. L. Scarf, R. W. Fredericks, and E. J. Smith, Initial results from the ISEE 1 and 2 plasma wave investigation, *Space Sci. Rev.*, *23*, 103–122, 1979.

Hayes, L. M., and D. B. Melrose, Generation of ordinary mode auroral kilometric radiation from extraordinary mode waves, *J. Geophys. Res.*, *91*, 211–217, 1986.

Helliwell, R. A., A theory of discrete VLF emissions from the magnetosphere, *J. Geophys. Res.*, *72*, 4773–4790, 1967.

Huff, R. L., W. Calvert, J. D. Craven, L. A. Frank, and D. A. Gurnett, Magnetic mapping of AKR sources to the aurora, *Eos Trans. AGU*, *67*, 1161, 1986.

Jones, D., Mode-coupling of *Z*-mode waves as a source of terrestrial kilometric and Jovian decametric radiations, *Astron. Astrophys.*, *55*, 245–252, 1977.

Jones, D., G. Gapper, and R. Herring, Auroral kilometric radiation from field-aligned plasma density enhancements, *Ann. Geophys.*, *2*, 95–104, 1984.

Kaiser, M. L., J. K. Alexander, A. C. Riddle, J. B. Pearce, and J. W. Warwick, Direct measurements by Voyagers 1 and 2 of the polarization of terrestrial kilometric radiation, *Geophys. Res. Lett.*, *5*, 857–860, 1978.

Kaiser, M. L., M. D. Desch, and S. A. Curtis, The sources of Uranus' dominant nightside radio emissions, *J. Geophys. Res.*, *92*, 15,169–15,176, 1987.

Le Queau, D., R. Pellat, and A. Roux, The maser synchrotron instability in an inhomogeneous medium: Application to the generation of the auroral kilometric radiation, *Ann. Geophys.*, *3*, 273–291, 1985.

Mellott, M. M., W. Calvert, R. L. Huff, D. A. Gurnett, and S. D. Shawhan, DE-1 observations of ordinary mode and extraordinary mode auroral kilometric radiation, *Geophys. Res. Lett.*, *11*, 1188–1191, 1984.

Mellott, M. M., R. L. Huff, and D. A. Gurnett, The auroral kilometric radiation: DE 1 direction finding studies, *Geophys. Res. Lett.*, *12*, 479–482, 1985.

Mellott, M. M., R. L. Huff, and D. A. Gurnett, DE 1 observations of harmonic auroral kilometric radiation, *J. Geophys. Res.*, *91*, 13,732–13,738, 1986.

Melrose, D. B., A phase-bunching mechanism for fine structures in auroral kilometric radiation and Jovian decametric radiation, *J. Geophys. Res.*, *91*, 7970–7980, 1986.

Melrose, D. B., R. G. Hewitt, and G. A. Dulk, Electron cyclotron maser emission: Relative growth and damping rates for different modes and harmonics, *J. Geophys. Res.*, *89*, 897–904, 1984.

Meng, C.-I., and R. E. Huffman, Ultraviolet imaging from space of the aurora under full sunlight, *Geophys. Res. Lett.*, *11*, 315–318, 1984.

Meng, C.-I., R. E. Huffman, F. Del Greco, and R. Eastes, UV images of dayside auroral oval, *Eos Trans. AGU*, *68*, 396, 1987.

Morioka, A., H. Oya, and S. Miyatake, Terrestrial kilometric radiation observed by satellite Jikiken (EXOS-B), *J. Geomagn. Geoelectr.*, *33*, 37–62, 1981.

Oya, H., and A. Morioka, Observational evidence of *Z* and *L-O* mode waves as the origin of auroral kilometric radiation from the Jikiken (EXOS-B) satellite, *J. Geophys. Res.*, *88*, 6189–6203, 1983.

Shawhan, S. D., and D. A. Gurnett, Polarization measurements of auroral kilometric radiation by Dynamics Explorer-1, *Geophys. Res. Lett.*, *9*, 913–916, 1982.

Shawhan, S. D., D. A. Gurnett, D. L. Odem, R. A. Helliwell, and C. G. Park, The plasma wave and quasi-static electric field instrument (PWI) for Dynamics Explorer A, *Space Sci. Instrum.*, *5*, 535–550, 1981.

Shepherd, G. G., C. D. Anger, J. S. Murphree, and A. V. Jones, Auroral intensifications in the evening sector observed by the Viking ultra violet imager, *Geophys. Res. Lett.*, *14*, 395–398, 1987.

Winglee, R. M., Fundamental and harmonic electron cyclotron maser emission, *J. Geophys. Res.*, *90*, 9663–9674, 1985.

Wu, C. S., and L. C. Lee, A theory of the terrestrial kilometric radiation, *Astrophys. J.*, *230*, 621–626, 1979.



R. F. Benson, Mail Code 692, NASA Goddard Space Flight Center, Greenbelt, MD 20771.

D. A. Gurnett, R. L. Huff, and M. M. Mellott, Department of Physics and Astronomy, University of Iowa, Iowa City, IA 52242.



(Received September 17, 1987;
revised February 10, 1988;
accepted March 17, 1988.)